

The hermaphrodite sperm/oocyte switch requires the *Caenorhabditis elegans* homologs of PRP2 and PRP22

Alessandro Puoti^{***} and Judith Kimble^{*}

^{*}Department of Biochemistry and Howard Hughes Medical Institute, University of Wisconsin, 433 Babcock Drive, Madison, WI 53706; and [†]Department of Zoology, University of Fribourg, Pérolles, CH-1700 Switzerland

Contributed by Judith Kimble, December 23, 1999

Sex determination in the hermaphrodite germ line of *Caenorhabditis elegans* is controlled posttranscriptionally. The switch from spermatogenesis to oogenesis relies on regulation of the *fem-3* sex-determining gene via a regulatory element in the *fem-3* 3' untranslated region. Previous work showed that at least six *mog* genes are required for repression by the *fem-3* 3' untranslated region, and that one of those genes, *mog-1*, encodes a DEAH-box protein. In this paper, we report the cloning of *mog-4* and *mog-5* and the finding that *mog-4* and *mog-5* also encode DEAH-box proteins. Our molecular identification of *mog-4* and *mog-5* relied on genetic mapping and transformation rescue and was confirmed by a missense mutation in each gene. A phylogenetic analysis revealed that the *C. elegans* MOG-1, MOG-4, and MOG-5 proteins are closely related to the yeast proteins PRP16, PRP2, and PRP22, respectively. In view of their effect on *fem-3* regulation and their homology to PRP16, PRP2, and PRP22, we propose that MOG-1, MOG-4, and MOG-5 are required for posttranscriptional regulation, perhaps by modifying the conformation of ribonucleoprotein complexes.

In *Caenorhabditis elegans*, the hermaphrodite produces sperm during the fourth larval stage and oocytes in the adult (1). Normally, the *fem-3* sex-determining gene promotes male fates transiently in the XX hermaphrodite germ line (2). In dominant regulatory *fem-3* mutants, the XX germ line is masculinized: sperm are made continuously and no oogenesis occurs (3). Molecular analyses of these *fem-3* gain-of-function (*gf*) mutations revealed the point mutation element (PME), a cis-acting regulatory element in the *fem-3* 3' untranslated region (UTR), that is required for the switch from spermatogenesis to oogenesis (4). Furthermore, the *fem-3* 3' UTR is sufficient to repress a reporter transgene and this repression is PME-dependent (5). These findings have led to a model in which *fem-3* is repressed posttranscriptionally to achieve the hermaphrodite switch from spermatogenesis to oogenesis in the XX germ line.

Six *mog* genes (*mog-1*–*mog-6*) are key regulators of the hermaphrodite sperm/oocyte switch and are also critical for PME-mediated repression in reporter assays (5–7). XX animals homozygous for mutations in any of these *mog* genes fail to switch from spermatogenesis to oogenesis. In addition, the *mog* genes are required maternally for embryogenesis. It is not yet clear whether the *mog* gene products act directly or indirectly to promote PME-repression. One clue is that *mog-1* encodes a member of the DEAH box protein family, suggesting that it acts at a posttranscriptional level (8).

In this study, we report that *mog-4* and *mog-5* encode proteins of the DEAH-box family. Because three of the six *mog* genes encode members of this same family (ref. 8 and this work), we explored all DEAH-box proteins in the *C. elegans* genome by phylogenetic analysis and by RNA-mediated interference (RNAi). We found that *mog-1*, *mog-4*, and *mog-5* are closely related to the yeast splicing factors PRP16, PRP2, and PRP22, respectively, and that they are the only *mog* genes that encode DEAH-box proteins.

Materials and Methods

Cloning *mog-4*. Initial mapping placed *mog-4* to the left of *unc-52* on chromosome II (6). C04H5.6, which encodes a DEAH-box

protein, resides in this region. Rescue was attempted with C04H5 or a 12.8-kb *XbaI*–*BstXI* subclone (pAP1) covering C04H5.6. DNA injected was 5 ng/ μ l of the C04H5 cosmid or pAP1, 30 ng/ μ l pRF4 roller DNA, and 70 ng/ μ l *Haemophilus influenzae* genomic DNA as carrier. The *H. influenzae* DNA was added to create a complex extrachromosomal array, which facilitates germline expression (9). Adults injected were *unc-4(e120) mog-4(q233)/mnC1*. The penetrance of *mog-4(q233)* was 100% at 20°C: all adults scored were Mog; no oocytes and a large excess of sperm ($n = >100$ worms scored). *Unc-4* progeny carrying either C04H5 or pAP1 as transgenes were scored for fertility; when fertile, such animals had low brood sizes and segregated many dead embryos, as expected for a weakly rescued *mog-4* mutant. From 29 worms injected, 86 F1 rollers were obtained. Among those rollers were seven sterile UncMog worms and three fertile Uncs, which were rescued. One fertile line was maintained for several generations. To confirm the identity of *mog-4* as C04H5.6, we sequenced the corresponding genomic DNA from *mog-4(q233)* mutants: genomic DNA was extracted from *mog-4* homozygotes and C04H5.6 amplified by PCR using Expand *Taq* DNA polymerase (Boehringer Mannheim). PCR products were sequenced directly and compared with published sequence.

Cloning *mog-5*. *mog-5* maps between *unc-85* and *dpy-10* (ref. 6 and this study); it is deleted by *mnDf4*, but not by *mnDf96* or *mnDf30*. EEED8.5, which was predicted to encode a DEAH-protein, resides in this region. Rescue was attempted with cosmid EEED8, pJK610 (a 7.4-kb *HindIII* subclone covering EEED8.5), or pJK611, a variant of pJK610 with a 2,344-nt deletion (a *BspEI* fragment). The composition of injected DNAs was similar to that described for *mog-4*, except with relevant DNAs. Adults injected were *mog-5(q449) dpy-10(e128)/unc-85(e1414)*; progeny were scored for fertile Dpy-10. On injection of 22 heterozygotes, 41 fertile Dpy were obtained of which 16 were rescued *mog-5* homozygotes and 25 were recombinants. Rescued mutants were distinguished from recombinants by their reduced fertility (3–100 eggs laid per individual) and reduced embryonic viability. A few stable rescued lines were obtained. Rescue (the number of fertile rolling Uncs/total rolling Uncs) was $\approx 80\%$ for *mog-5*, but $<35\%$ for *mog-4*, even though similar injection mixtures were used.

Isolation of cDNAs. *C. elegans* cDNA libraries (λ RB1 and λ RB2, provided by R. Barstead, Oklahoma Medical Research Foundation, Oklahoma City, OK) were screened with genomic *mog-4* and *mog-5* probes. To obtain 5' ends, we used a 380-nt *mog-4* probe from position –195 in the 5'-flanking region and to

Abbreviations: UTR, untranslated region; PME, point mutation element; fem, feminization; mog, masculinization of the germ line; PRP, pre-mRNA processing; RNAi, RNA-mediated interference.

[†]To whom reprint requests should be addressed. E-mail: alessandro.puoti@unifr.ch.

The publication costs of this article were defrayed in part by page charge payment. This article must therefore be hereby marked "advertisement" in accordance with 18 U.S.C. §1734 solely to indicate this fact.

position +185 in the coding region and a 257-nt *mog-5* probe (−92 to +171). For both genes, full-length cDNAs were obtained by joining cDNAs from the 3' end, obtained from an oligo(dT) primed library (λRB1), with cDNAs from the 5' end, obtained from a random-primed library (λRB2). The joining sites are *Aat*II in *mog-4* and *Eco*RI in *mog-5*. The full-length cDNA clones were cloned into the pBluescript vector (+KS, Stratagene) and sequenced by using standard procedures.

RNA Extraction and Northern Analysis. Poly(A)⁺ RNA was extracted from synchronized animals as described (8). Briefly, frozen worms were homogenized in buffer containing 200 μg/ml proteinase K (Boehringer Mannheim), poly(A)⁺ RNA adsorbed onto oligo(dT)cellulose (Pharmacia), and eluted under low salt conditions. Typically, 2–3 μg of denatured poly(A)-enriched RNA was loaded per lane and separated on a 1.2% denaturing glyoxal gel (10). RNA was blotted on a Hybond-N filter (Amersham) and probed as described (8).

RNA Interference. For each *mog* gene, a fragment of cDNA was cloned into pBluescript and used as a template for transcription with T3 or T7 RNA polymerase (Stratagene) [nt 247–799 for *mog-1*, nt 217–902 for *mog-4*, and nt 1–1451 for *mog-5*, with numbering starting at the initiator codon]. Similar regions were selected for other genes tested: positions 10,903–11,262 on F56D2; 23,941–24,323 on T05E8; and 38,040–38,468 on C06E1. Constructs were linearized and transcribed into cRNA according to the manufacturer's protocol (Stratagene mCAP RNA Capping kit). Antisense cRNA (1.5 μg/μl) was injected into wild-type adult hermaphrodites and progeny scored for phenotypes. Embryos not hatched >48 hr after laying were scored as dead. The time window of progeny scored starts 10 hr after injection and ends when no more embryos are produced (≈80 hr). To obtain double-stranded RNAs, strands were transcribed with T3 and T7 RNA polymerase (Stratagene), annealed, mixed equally in injection buffer (6.6 mM potassium phosphate, pH 7.3/1 mM potassium citrate, pH 7.5/0.66% polyethylene glycol 6000), and incubated for 10 min at 68°C and for 30 min at 37°C. RNA synthesis, annealing, and integrity were checked on a Tris-borate/EDTA agarose gel.

Phenotype Analysis. Germ cells were counted in XX adults of genotype *mog-4*, *unc-4 mog-4*, *mog-5*, or *mog-5 unc-4* mutants. Animals of 24–30 hr past L4 and raised at 20°C were stained by 4',6-diamidino-2-phenylindole (0.5 μg/ml in ethanol) and mature sperm nuclei counted in single gonadal arms. Numbers were similar in marked and unmarked mutants.

Results and Discussion

Cloning *mog-4* and *mog-5*. The *C. elegans* genome sequence (11) contains six members of the DEAH-box protein family; in addition, there are many members of the broader DEAD-box (or even more broadly DEXX-box) superfamilies, but these more divergent proteins are not considered here. One DEAH-box protein is *mog-1* (8). Each of two others mapped near other *mog* genes: C04H5.6 maps near *mog-4* and EEED8.5 near *mog-5* (Fig. 1A, Top and B, Top). To determine whether *mog-4* and *mog-5* might encode DEAH-box proteins, we attempted rescue of *mog-4* and *mog-5* homozygotes, which are normally sterile.

We found that C04H5 and a subclone of C04H5 (pAP1) predicted to encode only one transcript, C04H5.6, both rescued *mog-4*(*q233*) homozygotes to fertility (see *Materials and Methods*) (Fig. 1A Middle and Bottom). Rescue was not observed with pAP2, a variant of pAP1 bearing a deletion of 181 nt from the first exon (Fig. 1A Bottom); this deletion causes a frameshift, leading to a premature stop codon. Identification of *mog-4* as C04H5.6 was confirmed by sequencing the corresponding genomic DNA from *mog-4*(*q233*): this mutation is associated

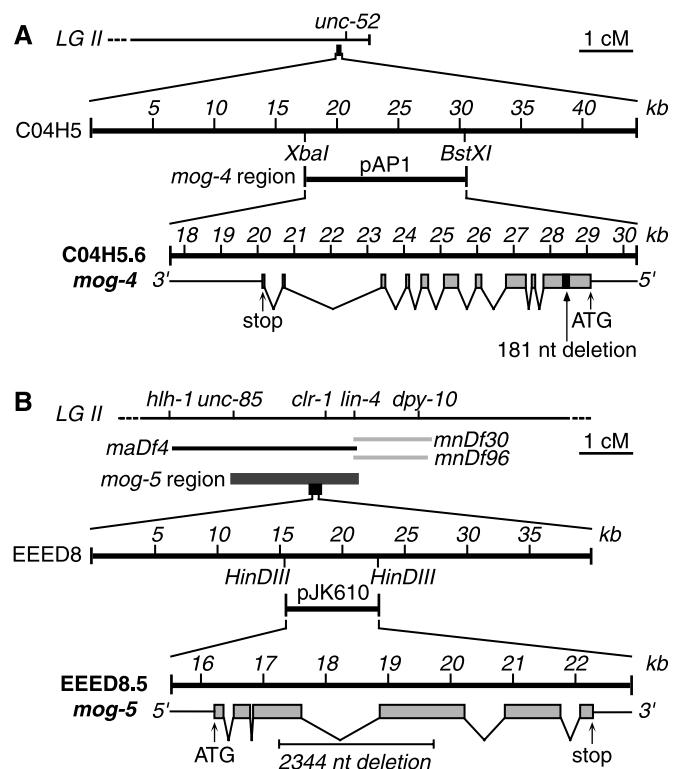


Fig. 1. Cloning *mog-4* and *mog-5*. (A) *mog-4*. (A, Top) Genetic map of *mog-4* region at right end of chromosome II (6). (A, Middle) Cosmid C04H5 resides ≈100 kb to the left of *unc-52*. The 12.8-kb subclone of C04H5, called pAP1, is predicted to contain only one transcript, C04H5.6. (A, Bottom) Exon/intron structure of C04H5.6, as predicted by Genefinder and confirmed by cDNA analysis (see *Material and Methods*). The 5' UTR and 3' UTR, thin lines; coding regions of exons, gray boxes; lines joining exons; predicted initiation (ATG) and stop codons are indicated. The pAP2 plasmid contains a 181-nt deletion (black box) from position +582 to +763 in the *mog-4* cDNA; this deletion shifts the reading frame and results in a premature stop codon. (B) *mog-5*. (B, Top) Genetic map of *mog-5* region in the center of chromosome II (ref. 6 and this work). Genetic mapping (see *Materials and Methods*) placed *mog-5* in a region corresponding to 2.4 cM or ≈30 cosmids on the physical map. (B, Middle) The EEED8 cosmid resides within the *mog-5* region. The pJK610 subclone of EEED8 is 7.4 kb and contains only EEED8.5, the transcript predicted to encode a DEAH-box protein. (B, Bottom) Exon/intron structure of EEED8.5, as predicted by Genefinder and confirmed by cDNA analysis (see *Material and Methods*). Diagram represented as in Fig. 1A. The pJK611 plasmid contains a 2,344-nt deletion from position 974–2,056 in the *mog-5* cDNA [or 1,200–3,544 in the *mog-5* genomic fragment]; this deletion removes parts of the third and fourth exons but retains the reading frame.

with a G to A transition at position 3,573 and creates a missense mutation (see below).

The results for *mog-5* were parallel to those obtained for *mog-4*: both the cosmid EEED8 and a 7.4-kb subclone, pJK610, which is predicted to encode only EEED8.5, rescued *mog-5*(*q449*) homozygotes to fertility (see *Materials and Methods*). By contrast, a plasmid with a 2344-nt deletion (*Bsp*EI) that removes 361 aa from MOG-5 did not rescue *mog-5*(*q449*). The identity of *mog-5* as EEED8.5 was confirmed by sequencing *mog-5*(*q449*): it is associated with a G to A transition at position 3,318, which creates a missense mutation (see below).

***mog-4* and *mog-5* mRNAs.** Both *mog-4* and *mog-5* are trans-spliced to the SL1 splice leader just before the first AUG (3 or 1 nt upstream for *mog-4* and *mog-5*, respectively). We suggest this first AUG to be the initiator codon because it generates an N terminus conserved among close homologs for both genes (see

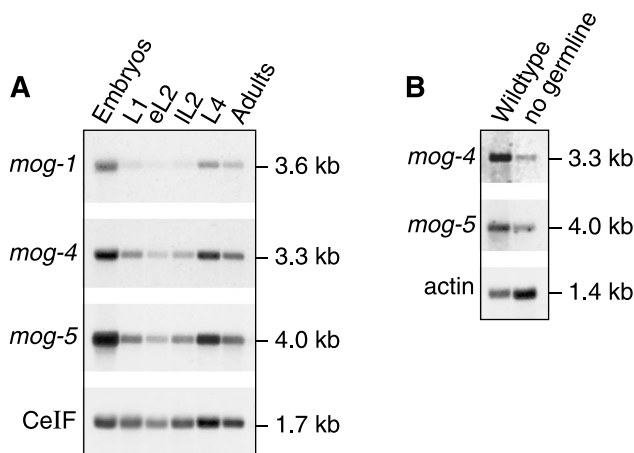


Fig. 2. *mog-4* and *mog-5* mRNA expression. (A) *mog-4* and *mog-5* RNAs during development. In each lane, 3.8 μ g of poly(A)-enriched RNA was loaded from embryos (E), larvae [first larval stage (L1), early L2 (eL2), late L2 (IL2), and fourth larval stage (L4)] and adults (A). Probes were the full-length cDNAs for *mog-4* (pAP5) and *mog-5* (pJK615), respectively. Molecular sizes were determined by comparison to Promega RNA markers. *CeIF* encodes the *C. elegans* homolog of eukaryotic initiation factor 4A, which is expressed at a constant level throughout development (28). (B) *mog-4* and *mog-5* RNAs are present in soma and germ line. RNA was derived from wild-type (N2) adults and *glp-1(q224)* adults raised at restrictive temperature, which have virtually no germ line (29). Each lane was loaded with 2.5 μ g of poly(A)-enriched RNA and probed with *mog-4*, *mog-5*, and *C. elegans* actin-1-specific (as loading control) cDNAs. The *mog-4* and *mog-5* transcripts are abundant in wild-type RNA but much reduced in animals lacking a germ line. For comparison, blots were also probed with *mog-1* (A and not shown).

below). The *mog-4* and *mog-5* cDNAs contain 3,211 and 3,731 nt, respectively, not including their poly(A) tails. At its 3' end, *mog-4* has a canonical poly(A) addition signal (AAUAAA) located 8 nt upstream of the poly(A) tail; *mog-5*, by contrast, possesses no well-recognized polyadenylation signal, as observed in $\approx 7\%$ of *C. elegans* transcripts (12).

Single transcripts of expected size were observed in Northern blots when probed for *mog-4* and *mog-5* mRNAs (Fig. 2A). These mRNAs are abundant in embryos, low in early larval development, and increased again in later larvae and adults (Fig. 2A). We next analyzed *mog-4* and *mog-5* mRNAs in poly(A)⁺ RNA derived from either wild-type adults (which possess $\approx 2,000$ germ cells) or *glp-1* mutant adults (which have only 16–32 sperm and no other germ cells) (Fig. 2B). The *mog-4* and *mog-5* mRNAs were abundant in wild-type adults but reduced in *glp-1* mutants. The simplest interpretation is that *mog-4* and *mog-5* mRNAs are expressed in the germ line as well as somatic tissues. This expression is consistent with the *mog* germline phenotype and with the somatic effect of *mog* genes in reporter assays (5). A similar expression also was observed for *mog-1* (8).

***mog-4* and *mog-5* Encode DEAH-Box Proteins.** The MOG-4 and MOG-5 polypeptides contain seven conserved motifs typical of members of the DEAH-box protein family (Fig. 3, black boxes) (13, 14). Although full-length MOG-4 and MOG-5 polypeptides share only 38.4% identity, a conserved region of 617 aa (including the seven motifs) is 55.5% identical. This conserved region extends from amino acid 357–974 in MOG-4 and is demarcated by arrows in Fig. 3. We refer to this conserved region as a “domain of high similarity” and used it for phylogenetic analyses (see below). Outside this domain, MOG-5 contains multiple serine-arginine (SR) and aspartic acid-arginine (DR) dipeptides (Fig. 3, thin underline), which define an RS domain (15). Such RS regions are also found in MOG-1 and in human homologs but not in MOG-4 or in PRP2, PRP16, PRP22, or PRP43 (see

below). In addition, MOG-5 contains a motif found in bacterial ribosomal protein S1 (Fig. 3, thick underline); this same motif is found in yeast PRP22 and its human homolog HRH1 (16, 17).

A DEAHER Subfamily of DEAH-Box Proteins. Using the BLASTP program, 15 proteins were identified as well-matched to MOG-1, MOG-4, and MOG-5: three additional proteins from *C. elegans* (F56D2.6, C06E1.10, and T05E8.3), four from *Saccharomyces cerevisiae* (PRP2, PRP16, PRP22, and PRP43), one from *Schizosaccharomyces pombe* (Cdc28), five from vertebrates [KIAA0057, hPRP16, HRH1, mDEAH9 (18), and DBP1 (19)], and two from *Arabidopsis thaliana* (helices 1 and 2; GenBank accession nos. X981340 and Z97341). A comparison of the “domains of high similarity” of these 18 proteins revealed features that were well conserved among a subset of 16 proteins (all but C06E1.10 and T05E8.3). Whereas all 18 possess the groups of amino acids shared by all DEAH-box proteins (Fig. 3, black boxes), the subset of 16 also share an additional 120 amino acids scattered throughout the “domain of high similarity” (Fig. 3, gray boxes). Among these are amino acids flanking the more broadly conserved amino acids: following DEAH is ER(T/S) in motif III, and preceding PRRVAA is TQ in motif Ia (already noted in ref. 14). In addition, the 16 share a common size in their domains of high similarity [the shortest is 593 aa (KIAA0057) and the longest is 640 aa (PRP2)]. The T05E8.3 protein shares 116/120 aa marked in gray (Fig. 3) and has several insertions into its domain of high similarity. Remaining homologs, including *C. elegans* C06E1.10, other DEAH proteins, such as the Bloom syndrome RecQ helicases (ref. 20 and for review see ref. 21), and other helicases belonging to the broader DEXH family [e.g., the *Drosophila* Homeless and Maleless proteins (22, 23)], are even further diverged. We propose that the shared features revealed by this comparison will prove useful and suggest the name DEAHER-box proteins to distinguish this class of proteins.

Critical Amino Acids in DEAHER-Box Proteins. The *mog-4* and *mog-5* mutations each alter a conserved residue. In *mog-4(q433)*, a conserved glycine (G) is changed to a serine (S) (Fig. 3, ○) in motif VII (QRXGRAGR), a motif involved in ATP hydrolysis in the DEAD-box protein eIF-4A (13). In yeast PRP16, an alanine substitution of glycine 691, which corresponds to the altered amino acid in *mog-4(q233)*, is not essential (24); however, the same amino acid is critical for catalytic activity of the vaccinia virus NPH-II DEVH-box protein (25). Although a change to serine might be more detrimental than one to alanine, *mog-4(q233)* is probably not a null allele (see below). In *mog-5(q449)*, a conserved glutamic acid (E) is changed to lysine (K) (Fig. 3, ●). Furthermore, in a *prp22* temperature-sensitive allele, a conserved glycine, which corresponds to amino acid 659 in MOG-4, is changed to glutamic acid (16). Finally, *mog-1(q473)* changes a conserved arginine [R702 in MOG-4] to histidine (H) (8). Therefore, all known missense mutations in the *mog* genes and close homologs alter conserved amino acids.

Null and Non-Null Mog Phenotypes. Among the four *mog-1* alleles examined previously, three were nonsense mutants predicted to be null, and one was a missense mutant (8). Intriguingly, the *mog-1* nonsense mutants were phenotypically distinguishable from the *mog-1(q473)* missense mutant. Both types of mutant failed in their switch to oogenesis, but the null mutants had an additional defect in germline proliferation (8). We have found that the germ lines of *mog-4(q233)* and *mog-5(q449)* missense mutants are comparable to that of the *mog-1* missense mutant with respect to germline proliferation: $1,073 \pm 341$ ($n = 18$) (8), 638 ± 173 ($n = 12$), or 775 ± 216 ($n = 10$) sperm per arm in *mog-1(q473)*, *mog-4(q233)*, and *mog-5(q449)*, respectively. By contrast, *mog-1* null mutants possessed ≈ 300 sperm per arm. The total germ cells (immature plus gametes) was also larger in

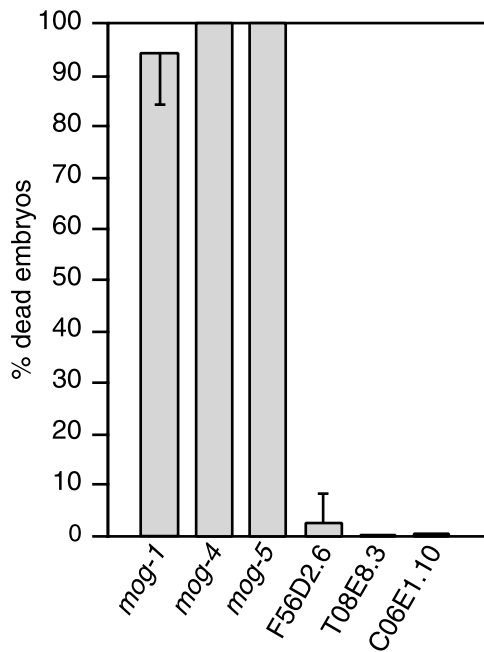


Fig. 4. RNA interference against *C. elegans* genes encoding DEAH-box proteins. Embryonic lethality observed after RNA interference directed against six *C. elegans* genes encoding DEAH-box proteins. Progeny were scored for arrested embryos 24 hr after eggs were laid. *mog-1*, $n = 756$; *mog-4*, $n = 600$; *mog-5*, $n = 276$; F56D2.6, $n = 629$; C06E1.10, $n = 929$; and T05E8.3, $n = 752$.

the missense mutants than in the *mog-1* null mutants. We therefore suggest that the *mog-4*(*q233*) and *mog-5*(*q449*) mutants may retain partial activity and that null alleles of *mog-4* or *mog-5* may cause a different phenotype, for instance embryonic or larval lethality.

Comparison of *C. elegans* DEAH-Box Proteins by RNA Interference. To compare functions of the *C. elegans* DEAH-box and DEAH-ER proteins, we used RNA interference (RNAi) to reduce gene function. For *mog-1*, *mog-4*, and *mog-5*, RNAi resulted in embryonic lethality (Fig. 4), which was expected: the *mog* genes are required maternally for embryogenesis (6, 7). Occasionally, embryos laid early after injection developed into sterile adults making only sperm. The *mog*(RNAi) embryos arrested at specific stages: *mog-1*(RNAi) embryos arrested with ≈ 300 cells at the early comma stage, whereas *mog-4*(RNAi) and *mog-5*(RNAi) embryos arrested earlier (166 ± 9 cells for *mog-4* and 130 ± 10 cells for *mog-5*) (not shown).

RNAi directed against the three remaining *C. elegans* DEAH-box proteins resulted in little or no embryonic lethality (Fig. 4). This same result was observed with either single-stranded (ss) antisense RNA (Fig. 4) or double stranded (ds) RNA (not shown). Furthermore, neither ssRNAi or dsRNAi progeny exhibited a Mog germ line. F56D2.6(dsRNAi) and C06E1.10(dsRNAi) progeny grew more slowly than normal and T05E8.3 had no obvious defect (not shown). We also compared the map positions of these DEAH-box genes to the other *mog* genes. The *mog-2* and *mog-6* genes map to chromosome II, whereas *mog-3* maps to the left of *dpy-17* on chromosome III (ref. 6 and A.P. unpublished data). By contrast, F56D2.6 maps to the right of *dpy-17* on chromosome III, T05E8.3 maps to chromosome I, and C06E1.10 maps to the center of chromosome III. Therefore, these three DEAH-box proteins do not map to any known *mog* gene and do not exhibit either the embryonic lethality or defective germline phenotypes typical of *mog* mu-

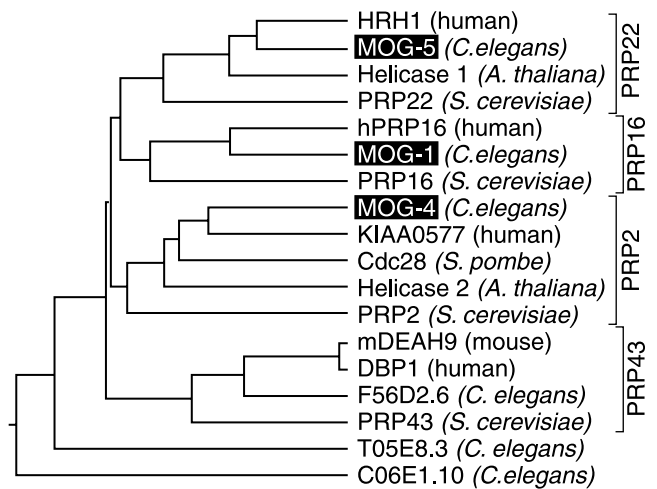


Fig. 5. Phylogenetic tree of DEAH-box proteins. Neighbor joining phylogram of the conserved region of 18 DEAH-box proteins. The region used to generate this phylogram lies between the two arrows in Fig. 3. The phylogram was obtained by the CLUSTAL method in the DNASTAR DNA analysis package. Similar results were obtained with an uncorrected distance matrix using the PILEUP algorithm (GCG, Madison, WI).

nants. We suggest that MOG-1, MOG-4, and MOG-5 define a functional subset of DEAH-box proteins within the *C. elegans* genome.

Phylogenetic Analysis of DEAH-Box Proteins. To investigate the evolutionary relationships among the 18 most similar DEAH-box proteins of different species, we compared their “domains of high similarity” (Fig. 3, region between arrows) using the CLUSTAL method (DNASTAR) and GCG PILEUP programs (Fig. 5; not shown). This analysis identified four clusters for the DEAH-ER subset of DEAH-box proteins, each containing a well-characterized PRP protein from *S. cerevisiae* (Fig. 5). The only proteins not falling into one of these clusters were T05E8.3 and C06E1.10 (Fig. 5), which also did not conform to the DEAH-ER family definition. Two additional *C. elegans* proteins, T07D4.3 and F52B5.3, are much more diverged and beyond the scope of this work.

The clustering of DEAH-ER proteins into four groups, which was based on their domains of high similarity (Fig. 3, region between arrows), is supported by similarities in other parts of the proteins as well. Unique to the PRP16 group is the DR[E/D]WY[D/M][N/M][D/E] motif (at position 230 and 171 in MOG-1 and PRP16, respectively) (8). Distinctive to the PRP22 group is a conserved S1 domain in the N terminus (Fig. 4, thick underline). A shared feature of the PRP43 group is their short overall length: PRP43, mDEAH9, DBP1, and F56D2.6 have 767, 758, 813, and 739 amino acids respectively versus averages of 1171, 1133, and 955 for the PRP22, PRP16, and PRP2 groups. Although no specific motif or unique feature was discerned for the PRP2 group, MOG-4 was closely related to KIAA0057 (both lack an RS domain, have 68.8% identity in the region of high similarity and 53.9% identity throughout the entire peptide).

We conclude that MOG-1 is closely related to PRP16, MOG-4 to PRP2, and MOG-5 to PRP22. Indeed, a search of the entire *C. elegans* genome reveals no better homologs. The idea that MOG-1, MOG-4, and MOG-5 are the *C. elegans* homologs of yeast proteins PRP16, PRP2, and PRP22, respectively, is supported by comparison with the human homologs hPRP16 and HRH1, which are even more similar to the *C. elegans* proteins than to the proposed yeast homologs (17, 26). We tried to rescue *prp16* and *prp22* mutants with the respective *C. elegans mog-1* and

mog-5 cDNAs, but were unsuccessful (A.P. unpublished data). This failure to complement the yeast mutants was, however, predictable because rescue of *prp16* with hPRP16 was only possible with a human-yeast chimeric gene (26). Similarly, HRH1 was barely able to complement a temperature-sensitive *prp22* mutant strain at 32°C (17).

In yeast, PRP16, PRP2, and PRP22 are integral components of the spliceosomal machinery (27). However, in *C. elegans*, the biochemical functions of MOG-1, MOG-4, and MOG-5 remain unknown. Although a role for the *mog* genes in splicing remains possible, no general splicing defect was observed in *mog-1* null mutants (8). Furthermore, the *mog* genes are required for PME-repression of reporter transgenes (5). One explanation of these apparently disparate results is that the *mog* genes, although evolutionarily related to the yeast PRP genes, have acquired a different function. One speculative idea is that the MOG proteins may promote a conformational change or the disassembly

of a ribonucleoprotein complex required for PME-mediated repression. Alternatively, the PRP16, PRP2, and PRP22 proteins in yeast may function more broadly than previously thought and modulate a variety of ribonucleoprotein complexes, including those integral to splicing.

We are grateful to Jim Dahlberg, Phil Anderson, Betsy Goodwin, and Eric Haag for comments on the manuscript. We thank the *C. elegans* Sequencing Consortium for providing *C. elegans* genome sequence before publication and Alan Coulson for cosmids. We are grateful to R. Barstead for cDNA libraries and to the *Caenorhabditis* Genetics Center and Theresa Stiernagle for *C. elegans* strains. We thank Laura Vanderploeg for figure preparation. A.P. was supported by the European Molecular Biology Organization and the Howard Hughes Medical Institute. J.K. is an investigator with the Howard Hughes Medical Institute. This work was in part supported by Swiss National Science Foundation Grants 823A-042914, 3100-055384.98/1, and 3130-054989.98/1 (to A.P.).

- Schedl, T. (1997) in *C. elegans II*, eds. Riddle, D. L., Blumenthal, T., Meyer, B. J. & Priess, J. R. (Cold Spring Harbor Laboratory Press, Plainview, NY), pp. 241–269.
- Hodgkin, J. (1986) *Genetics* **114**, 15–52.
- Barton, M. K., Schedl, T. B. & Kimble, J. (1987) *Genetics* **115**, 107–119.
- Ahringer, J. & Kimble, J. (1991) *Nature (London)* **349**, 346–348.
- Gallegos, M., Ahringer, J., Crittenden, S. & Kimble, J. (1998) *EMBO J.* **17**, 6337–6347.
- Graham, P. L., Schedl, T. & Kimble, J. (1993) *Dev. Genet. (Amsterdam)* **14**, 471–484.
- Graham, P. L. & Kimble, J. (1993) *Genetics* **133**, 919–931.
- Puoti, A. & Kimble, J. (1999) *Mol. Cell. Biol.* **19**, 2189–2197.
- Kelly, W. G., Xu, S., Montgomery, M. K. & Fire, A. (1997) *Genetics* **146**, 227–238.
- Sambrook, J., Fritsch, E. F. & Maniatis, T. (1989) *Molecular Cloning: A Laboratory Manual* (Cold Spring Harbor Lab. Press, Plainview, NY), 2nd Ed.
- The *C. elegans* Sequencing Consortium (1998) *Science* **282**, 2012–2018.
- Blumenthal, T. & Steward, K. (1997) in *C. elegans II*, eds. Riddle, D. L., Blumenthal, T., Meyer, B. J. & Priess, J. R. (Cold Spring Harbor Lab. Press, Plainview, NY), pp. 117–145.
- Pause, A. & Sonenberg, N. (1992) *EMBO J.* **11**, 2643–2654.
- Arenas, J. E. & Abelson, J. N. (1997) *Proc. Natl. Acad. Sci. USA* **94**, 11798–11802.
- Fu, X.-d. (1995) *RNA* **1**, 663–680.
- Company, M., Arenas, J. & Abelson, J. (1991) *Nature (London)* **349**, 487–493.
- Ono, Y., Ohno, M. & Shimura, Y. (1994) *Mol. Cell. Biol.* **14**, 7611–7620.
- Gee, S., Krauss, S. W., Miller, E., Aoyagi, K., Arenas, J. & Conboy, J. G. (1997) *Proc. Natl. Acad. Sci. USA* **94**, 11803–11807.
- Imamura, O., Sugawara, W. & Furuichi, Y. (1997) *Biochem. Biophys. Res. Commun.* **240**, 335–340.
- Ellis, N. A., Groden, J., Ye, T. Z., Straughen, J., Lennon, D. J., Ciocci, S., Proytcheva, M. & German, J. (1995) *Cell* **83**, 655–666.
- Kusano, K., Berres, M. E. & Engels, W. R. (1999) *Genetics* **151**, 1027–1039.
- Kuroda, M. I., Kernan, M. J., Kreber, R., Ganetzky, B. & Baker, B. S. (1991) *Cell* **66**, 935–947.
- Gillespie, D. E. & Berg, C. A. (1995) *Genes Dev.* **9**, 2495–2508.
- Hotz, H.-R. & Schwer, B. (1998) *Genetics* **149**, 807–815.
- Gross, C. H. & Shuman, S. (1996) *J. Virol.* **70**, 1706–1713.
- Zhou, Z. & Reed, R. (1998) *EMBO J.* **17**, 2095–2106.
- Burge, C. B., Tuschl, T. & Sharp, P. A. (1999) in *The RNA World*, eds. Gesteland, R. F., Cech, T. R. & Atkins, J. F. (Cold Spring Harbor Lab. Press, Plainview, NY), 2nd Ed.
- Roussell, D. L. & Bennett, K. L. (1992) *Nucleic Acids Res.* **20**, 3783.
- Austin, J. & Kimble, J. (1987) *Cell* **51**, 589–599.